



Photoactivatable Prodrugs Hot Paper



Cyclometalated Gold(III)-Hydride Complexes Exhibit Visible Light-Induced Thiol Reactivity and Act as Potent Photo-Activated Anti-Cancer Agents

Hejiang Luo, Bei Cao, Albert S. C. Chan, Raymond Wai-Yin Sun, and Taotao Zou*

Abstract: The specific gold-sulfur binding interaction renders gold complexes as promising anti-cancer agents that can potentially overcome cisplatin resistance; while their unbiased binding towards non-tumoral off-target thiol-proteins has posed a big hurdle to clinical application. Herein we report that cyclometalated gold(III) complexes bearing hydride ligands are highly stable towards thiols in the dark but can efficiently dissociate the auxiliary hydride moiety and generate a gold-thiol adduct when excited with visible light. In consequence, the photo-activated gold(III) complexes potently inhibited thioredoxin reductase in association with up to > 400-fold increment of photocytotoxicity (vs. dark condition) without deactivation by serum albumin and along with strong anti-angiogenesis activity in zebrafish embryos. Importantly, the gold(III)-hydride complexes could be activated by two-photon laser irradiation at the phototherapeutic window as effectively as blue-light irradiation.

Introduction

There has been a burgeoning interest in developing gold-based anti-cancer therapeutics due to their intriguing mechanism-of-action that is different from cisplatin.^[1] Both gold(I) and gold(III) have proven specificity to target proteins/enzymes containing thiol (cysteine) or selenol (selenocysteine) moieties (e.g., thioredoxin reductase), leading to potent cytotoxicity towards cancer cells, including cisplatin-resistant variants.^[2] However, reactive gold complexes can also strongly bind a number of off-target thiols present in non-tumoral regions (such as serum albumin in blood and thiol-

enzymes in normal cells), which largely hampered their anti-cancer potency and also caused devastating side effects in vivo.^[1d,f,2b,3] In previous works, ligands such as N-heterocyclic carbene (NHC),^[4] phosphine,^[5] alkyne,^[3a,6] dithiocarbamate^[7] and thiourea^[8] containing different substituents have been employed to tune the thiol-reactivity of gold(I) and gold(III) complexes with some of them showing impressive in vivo anti-tumor activities. Nevertheless, it remains a big challenge to design gold complexes having a controllable thiol reactivity capable of inhibiting thiol-enzyme target(s) specifically in cancer cells with minimal effects on normal cells.

Photoactivatable metal anti-cancer prodrugs,^[9] in which the activity is triggered by ligand dissociation or photochemical reduction, have been demonstrated to show high tumor specificity.^[10] For example, Sadler and co-workers developed an organometallic $[(\eta^6\text{-}p\text{-cymene})\text{Ru}(\text{bmp})(\text{py})]^{2+}$ (bmp = 2,2'-bipyrimidine) complex that could selectively photo-dissociate the pyridine moiety and form an aqua derivative for DNA binding.^[11] Moreover, several Pt^{IV} prodrugs have been reported to be photochemically^[12] or photocatalytically^[13] activated to generate active Pt^{II} species able to bind DNA. In the literature, cyclometalated $[\text{Au}^{\text{III}}(\text{C}^{\wedge}\text{N}^{\wedge}\text{C})\text{L}]$ ($\text{H}_2\text{C}^{\wedge}\text{N}^{\wedge}\text{C}$ = 2,6-diphenylpyridine) complexes have shown potent activity for TrxR inhibition via ligand-thiol exchange reactions (when L = phosphine, pyridine, Cl or other labile ligands),^[14] whereas those with strong σ -donor ligands (such as NHC, alkyl, alkyne) resulted in high thiol-stability without suppression of TrxR.^[15] In view that hydride is a strong σ -donor and its associated metal complexes have shown potential photo-reactivity,^[16] we conceive the hydride-bearing cyclometalated gold(III) complexes may be developed as photoactivatable prodrugs. Herein we report a series of $[\text{Au}^{\text{III}}(\text{C}^{\wedge}\text{N}^{\wedge}\text{C})\text{H}]$ complexes that are stable against thiols in the dark but exhibit visible-light-induced thiol-reactivity and can act as photo-activated anti-cancer agents under in vitro and in vivo conditions. To the best of our knowledge, this is the first example of photoactivatable gold-based prodrugs with controllable thiol-reactivity.

Results and Discussion

The gold(III) hydride complexes **1a–1d** (Figure 1) were prepared following a modified literature procedure^[17] by treating $[\text{Au}^{\text{III}}(\text{C}^{\wedge}\text{N}^{\wedge}\text{C})\text{Cl}]$ with LiAlH_4 at -78°C , with products purified by column chromatography (see Supporting Information for synthesis and characterization details). In the ^1H NMR spectrum, these complexes show typical hydride

[*] H. Luo, Prof. Dr. A. S. C. Chan, Prof. Dr. T. Zou
Guangdong Key Laboratory of Chiral Molecule and Drug Discovery,
School of Pharmaceutical Sciences, Sun Yat-Sen University
Guangzhou 510006 (P. R. China)
E-mail: zoutt3@mail.sysu.edu.cn

Dr. B. Cao
Warshel Institute for Computational Biology, and General Education
Division, The Chinese University of Hong Kong
Shenzhen 518172 (P. R. China)

Prof. Dr. R. W.-Y. Sun
Guangzhou Lee & Man Technology Company Limited
Guangzhou 510000 (P. R. China)

Prof. Dr. T. Zou
State Key Laboratory of Coordination Chemistry, Nanjing University
Nanjing 210093 (P. R. China)

Supporting information and the ORCID identification number(s) for the author(s) of this article can be found under:
<https://doi.org/10.1002/anie.202000528>.

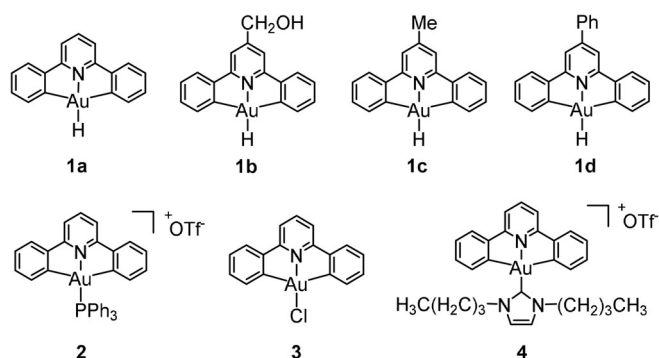


Figure 1. Chemical structures of the gold(III)-hydride complexes **1a**–**1d** and the related gold(III) complexes **2**–**4** for comparative study.

signals at $\delta = -6.57$ to -6.51 ppm in CDCl_3 . The ^1H - ^1H NOESY and COSY NMR spectra of **1a** are shown in Figure S1 in the Supporting Information. Complexes **1a**–**1d** are well soluble in common organic solvents such as CH_2Cl_2 , CHCl_3 , THF, DMSO and DMF, with a solubility of $> 10 \text{ mg mL}^{-1}$. The photo-reactivity of gold(III)-hydride complexes were initially examined (Figure 2). In the dark, these

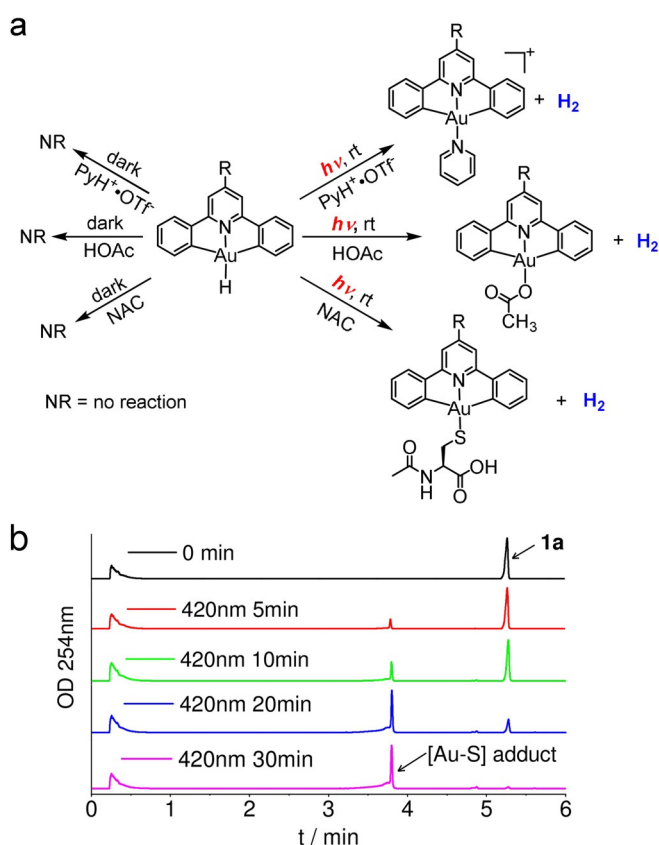


Figure 2. a) Reactions of **1a/1b** with $\text{PyH}^+\cdot\text{OTf}^-$, HOAc and NAC in CH_3CN or DMSO under dark/light conditions. For reactions with $\text{PyH}^+\cdot\text{OTf}^-$ and HOAc, the two solvents (CH_3CN and DMSO) gave similar yield for adduct formation. NAC is insoluble in CH_3CN and therefore only DMSO was used. b) LC diagram for the mixture of **1a** (1 mM) with 10-fold NAC in DMSO after 420 nm light irradiation for different time.

complexes display low hydricity with no reaction against 10-fold excess (10 mM) of pyridinium triflate ($\text{PyH}^+\cdot\text{OTf}^-$) and acetic acid.^[18] Interestingly, after 365 nm light irradiation (6.87 mW cm^{-2})^[19] for 10 min, a clean peak with a retention time of 3.88 min in the liquid chromatogram was detected for the mixture of **1a** with $\text{PyH}^+\cdot\text{OTf}^-$ in DMSO ($\approx 10\%$ yield, Figure S2a), which was identified to be $[\text{Au}^{\text{III}}(\text{C}^{\wedge}\text{N}^{\wedge}\text{C})\text{Py}]^+$ based on ESI-MS analysis (Figure S2b; **1b** gave similar results); further 365 nm light irradiation did not increase the yield and the solution became dark colored. By using ^1H NMR spectroscopy, a singlet peak at 4.62 ppm was detected in $[\text{D}_6]\text{DMSO}$, but disappeared after shaking the NMR tube (Figure S3), appearing to be H_2 formation.^[20] In the case of **1a** with 10-fold HOAc (10 mM) in CD_3CN , H_2 formation (4.57 ppm) is more obvious after 365 nm light irradiation (Figure S4). Simply using the H_2 content detected in the solution by ^1H NMR spectroscopy, the yield is calculated to be $\approx 40\%$ after 25 min irradiation. The adduct $[\text{Au}^{\text{III}}(\text{C}^{\wedge}\text{N}^{\wedge}\text{C})\text{OAc}]$ was also detected in the reaction mixture by ESI-MS (Figure S5). Both results suggest a photo-induced hydride transfer process.^[16a,21]

Subsequently, the stability/photo-reactivity of **1a** towards bio-relevant thiols was examined. Similarly, **1a** was stable with no change of the ^1H NMR spectrum in the presence of 10-fold (10 mM) excess of N-acetyl cysteine (NAC) after 72 h incubation (Figure S6). Notably, **1a** (1 mM) efficiently generated a single peak with a retention time of 3.78 min in the LC chromatogram ($> 90\%$ yield) after either 420 nm (11.10 mW cm^{-2} , completed within 30 min, Figure 2b) or 365 nm (completed within 15 min, Figure S7) light irradiation, which was identified to be the $[\text{Au-S}]$ adduct of $[\text{Au}^{\text{III}}(\text{C}^{\wedge}\text{N}^{\wedge}\text{C})\text{S}(\text{NAC})]$ based on LC-MS analysis ($m/z = 589.1$, Figure S8). Such efficiency is significantly higher than that towards $\text{PyH}^+\cdot\text{OTf}^-$ and HOAc. Also, H_2 was detected as revealed from ^1H NMR spectroscopy (4.62 ppm in $[\text{D}_6]\text{DMSO}$, Figure S9) and GC analysis (retention time 2.70 min, Figure S10). At a 100 μM concentration, **1a** is more photo-reactive with complete conversion within 10 min after 365 nm irradiation (Figure S11). The photo-substitution quantum yield is calculated to be 7.1×10^{-4} (Figure S12).

To elucidate the possible mechanism for the photo-reactivity of **1a**, density functional theory (DFT) and time-dependent DFT calculations were performed by using generalized gradient approximation exchange-correlation density functional PW91 and basis set of 6-31G* except SDD for Au. As shown in Table S1, the HOMO is composed of 12.6% d(Au), 60.1% $\pi(\text{Ph} + \text{Ph}')$ and 27.2% $\pi(\text{Py})$. The LUMO mainly consists of 24.4% $\pi^*(\text{Ph} + \text{Ph}')$ and 68.7% $\pi^*(\text{Py})$. Therefore, the excited state could be assigned to intraligand phenyl to pyridyl transition mixed with a minor metal to ligand charge transfer transition.^[22] Noticeably, from ground-state (S_0) to the lowest triplet excited-state (T_1), the bond length of Au–N(Py) and the two Au–C(Ph) shortens by 0.032 Å and 0.025 Å, respectively, via π interaction in LUMO orbital (Figure 3), indicative of stronger bonding at the excited state. In contrast, the Au–H bond, which is at the *trans* position of Au–N(Py), weakens with increase in bond length (0.008 Å) at the T_1 state, suggestive of the photo-lability of the $\text{Au}^{\text{III}}\text{–H}$ bond upon light irradiation.

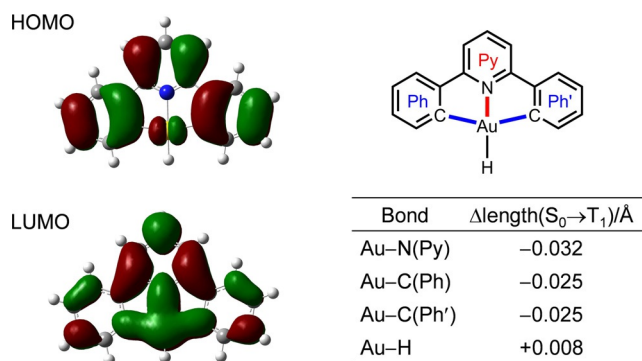


Figure 3. HOMO and LUMO orbital of **1a** (left, isovalue = 0.02) and bond length change from ground state (S_0) to the lowest triplet excited state (T_1).

We then tested whether the photo-induced thiol-reactivity can happen in aqueous solution. Complex **1a** (100 μM) was incubated with NAC (10 mM) in H_2O containing 20% DMF (v/v); no change of **1a** was found after 48 h based on LC-MS analysis (Figure S13). After irradiation with 365 nm light, efficient generation of $[\text{Au}^{\text{III}}(\text{C}^{\wedge}\text{N}^{\wedge}\text{C})\text{S}_{(\text{NAC})}]$ was identified (> 90% conversion in 30 min, Figure S14). Similar results were obtained in PBS-containing solution (Figure S15a) or by using glutathione as thiols (Figure S15b), showing that the gold(III)-hydride complexes maintained the photo-reactivity towards thiols under physiological-like condition.

Then we examined their activity toward TrxR inhibition. Complex **1b** was used, which displays a similar thiol reactivity (Figure S16) but a higher water solubility. The gold complexes were firstly incubated with recombinant rat TrxR1 in the presence of NADPH for 1 h, and then the enzyme catalyzed reaction was initiated by adding 5,5'-dithiobis-(2-nitrobenzoic acid) (DTNB) as substrates. As shown in Table 1, in dark condition, **1b** showed no inhibition at 100 nM. However, this complex potently suppressed TrxR with IC_{50} of 7.52 ± 1.43 nM after 365 nm irradiation for 5 min, which is comparable to **2** $[\text{Au}(\text{C}^{\wedge}\text{N}^{\wedge}\text{C})\text{PPh}_3]^+$ ($\text{IC}_{50} = 6.38 \pm 0.36$ nM) and **3** $[\text{Au}(\text{C}^{\wedge}\text{N}^{\wedge}\text{C})\text{Cl}]$ ($\text{IC}_{50} = 4.83 \pm 0.07$ nM) containing labile auxiliary ligands (Table 1), suggestive of efficient photo-induced breakage of the Au–H bond. For comparison, complex **4** $[\text{Au}(\text{C}^{\wedge}\text{N}^{\wedge}\text{C})\text{NHC}]^+$ containing a stable Au–C_(NHC) bond, did not show TrxR inhibition with $\text{IC}_{50} > 100$ nM. Subsequently,

Table 1: The effects of gold complexes on the inhibition of purified or cellular thioredoxin reductase.

Complex	TrxR inhibition	
	Recombinant TrxR1 [nM]	Cellular enzyme [μM] ^[b]
1b (dark)	> 100	> 20
1b (light) ^[a]	7.52 ± 1.43	1.68 ± 0.62
2	6.38 ± 0.36	1.24 ± 0.31
3	4.83 ± 0.07	n.d.
4	> 100	> 20
Auranofin	n.d.	1.20 ± 0.25

[a] 365 nm light irradiation for 5 min after incubation. [b] The cellular TrxR activity was estimated by using DTNB as substrates. n.d. = not determined.

their activity on cellular TrxR was performed by treating human liver hepatocellular carcinoma (HepG2) cells with gold complexes and was assayed using cell lysates. Results showed that **1b** displayed potent inhibition with IC_{50} of 1.68 ± 0.62 μM , similar to that of **2** ($\text{IC}_{50} = 1.24 \pm 0.31$ μM) and the potent TrxR inhibitor auranofin ($\text{IC}_{50} = 1.20 \pm 0.25$ μM). Again, **1b** in dark and **4** did not display obvious TrxR inhibition at the highest concentration we used (20 μM).

Based on the photo-induced thiol-reactivity, it is envisioned that the cellular TrxR inhibition is induced by covalent (coordinative) binding with cellular proteins. We verified this hypothesis by measuring the covalently bound gold content after incubating HepG2 cells with 1 μM of **1b** for 1 h, followed by further 5 min light irradiation. ICP-MS analysis of the gold content in acetone-precipitated cell lysates showed 91.7 ng Au per 10^6 cells after 365 nm light irradiation, which is 3.8-fold higher than that in dark conditions (24.2 ng Au per 10^6 cells). Additionally, since the $\text{Au}^{\text{III}}\text{-H}$ complexes are emissive (Figure 4a), its cellular localization was examined by confocal laser scanning microscopy (CLSM), which showed **1b** mainly localized in cytoplasm instead of the nucleus (Figure 4b). Such result is consistent with its potent cellular TrxR inhibition since both TrxR1 and TrxR2 are cytoplasmic enzymes.^[23] It is worth noting that the cells after 405 nm light excitation by CLSM displayed significant morphology changes typical of apoptosis (Figure 4c), including shape shrinkage, membrane blebbing, and phagocytosis by neighboring cells.^[24] We then used live/dead co-staining experiments to study the photo-activity by using the greenly-fluorescent calcein AM to indicate esterase activity of live cells and redly emissive ethidium homodimer-1 (EthD-1) to indicate damaged plasma membrane of dead cells. As shown in Figure 4e–h, the region after 2-min 405 nm laser irradiation displays red emission without green color, whereas the surrounding non-irradiated region exhibits green color with no red emission (the 405 nm laser itself does no harm to cancer cells, Figure S17). Therefore, the gold(III)-hydride complexes, after light irradiation, are able to attenuate cellular TrxR activity and to activate apoptosis-related cell death.

Subsequently, the dark- and photo-cytotoxicity of the gold(III)-hydride complexes towards human colon carcinoma (HCT116), lung carcinoma (A549), breast adenocarcinoma (MCF-7), and hepatocellular carcinoma (HepG2) was examined by MTT assay.^[25] All complexes are non-toxic in dark conditions with $\text{IC}_{50} > 100$ μM after 48 h incubation (Table 2 and Table S2–4). Instead, after a short 5 min 365 nm light irradiation, the cytotoxicity of **1a–1d** significantly increased with IC_{50} ranging from 0.24 to 5.86 μM , suggestive of up to > 400-fold stronger cytotoxicity. Under visible 420 nm irradiation for 10 min, these complexes are strongly cytotoxic as well, with IC_{50} of 0.95–16.8 μM . Shining a longer-wavelength light at 460 nm also induced cytotoxicity in the case of **1b**, **1c** and **1d**; in particular, **1d** which has a significantly red-shifted absorption (Figure S18), shows an IC_{50} of 5.43 μM (for HCT116) by 460 nm irradiation, which is still > 18-fold stronger than dark conditions.

We further examined whether the photo-induced cytotoxicity involves direct generation of singlet oxygen ($^1\text{O}_2$) or

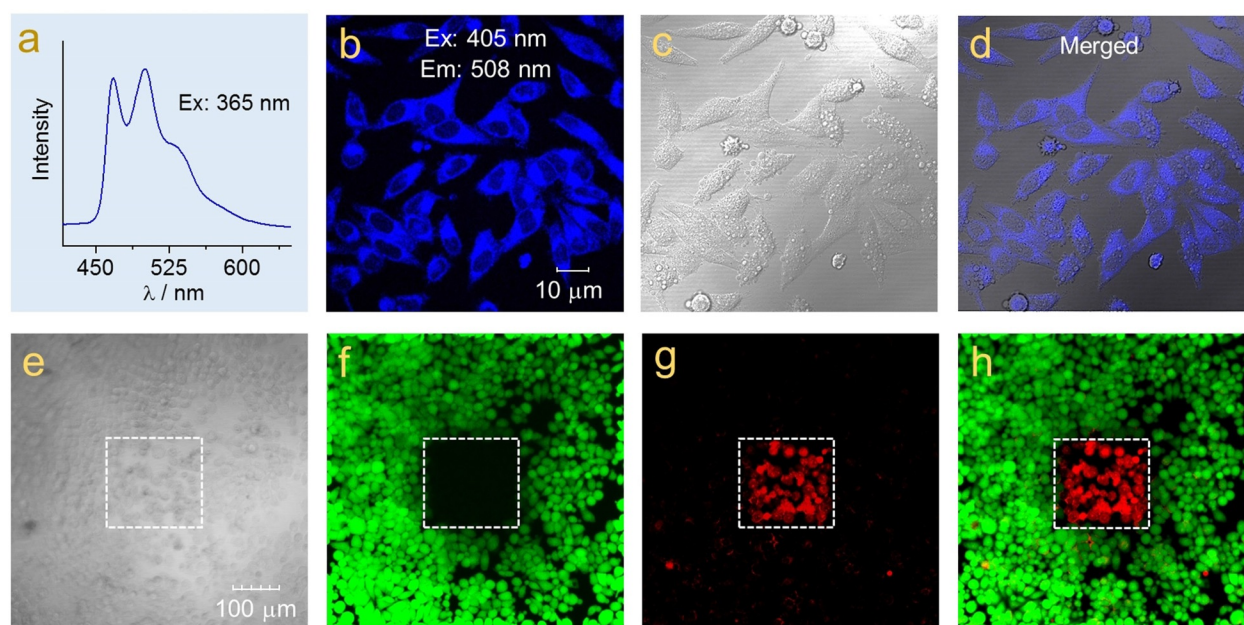


Figure 4. a) Emission spectrum of **1b** in dichloromethane. b) Fluorescence microscopy image of HepG2 cells treated with $10\ \mu\text{M}$ of **1b** for 1 h. c) Bright field showing characteristics of apoptotic morphology change after irradiation. d) Merged image. e–h) Fluorescent images of HepG2 cells treated with $10\ \mu\text{M}$ of **1b** for 1 h followed by 405 nm laser irradiation at selected region (dashed box) for 2 min. e) bright field; f) green channel; g) red channel; h) merged fluorescent image.

Table 2: Photo-cytotoxicity IC_{50} [μM] of gold(III)-hydride complexes after light irradiation at different wavelength. HCT116 cells were treated with gold(III) complexes for 1 h and then irradiated with light for 5 or 10 min. The cytotoxicity was measured after a total 48 h incubation.

Complex	Conditions			
	In dark	365 nm ^[a]	420 nm ^[b]	460 nm ^[b]
1a	> 100	1.01 ± 0.34	1.53 ± 0.75	> 50
1b	> 100	0.30 ± 0.15	1.22 ± 0.61	10.8 ± 3.0
1c	> 100	0.95 ± 0.10	2.31 ± 1.25	13.7 ± 4.5
1d	> 100	5.86 ± 0.28	1.45 ± 0.64	5.43 ± 2.69
auranofin	2.23 ± 0.15	4.71 ± 0.36	4.01 ± 0.47	1.81 ± 0.16
cisplatin	9.66 ± 3.29	28.0 ± 1.1	11.0 ± 0.4	14.0 ± 2.0

[a] 5 min irradiation; [b] 10 min irradiation. In all cases, the control group (with no drug treatment) did not show obvious cytotoxicity under light irradiation.

other reactive oxygen species such as hydroxyl radical (HO^\bullet). HepG2 cells were co-treated with **1a** and the $^1\text{O}_2$ suppressor NaN_3 (5 mM) or the HO^\bullet scavenger d-mannitol (50 mM), and then subjected to 365 nm light irradiation; a total 48 h incubation resulted in cytotoxic IC_{50} of $3.81 \pm 0.52\ \mu\text{M}$ for **1a** + NaN_3 , and $1.26 \pm 0.31\ \mu\text{M}$ for **1a** + d-mannitol, which are comparable to the photocytotoxicity of **1a** ($\text{IC}_{50} = 1.34 \pm 0.65\ \mu\text{M}$) under similar conditions, indicative of little to low photo-generated ROS. Therefore, the photocytotoxicity of gold(III)-hydride complexes could be attributed to photo-activated thiol reactivity rather than photosensitizing property.

Serum albumin is the major off-target thiol whose presence would lower the bioavailability of reactive gold to tumor cells. We tested if our photo-activation approach can help to decrease the influence of serum albumin by measuring the cytotoxicity in minimal essential medium (MEM) in the

presence/absence of bovine serum albumin (BSA, $40\ \text{mg mL}^{-1}$). Consistent with previous reports,^[4g] while auranofin is strongly cytotoxic in a medium without BSA ($\text{IC}_{50} = 0.19\ \mu\text{M}$), its cytotoxicity decreased dramatically in the BSA-containing medium with $\text{IC}_{50} = 13.2\ \mu\text{M}$ that is only 1.4 % of its original cytotoxicity (i.e., BSA-free condition, Figure 5). Likewise, the cytotoxicity of thiol-reactive **2** dropped by $\approx 90\%$ from $\text{IC}_{50} = 1.57\ \mu\text{M}$ in BSA-free medium to $16.23\ \mu\text{M}$ in MEM with BSA. Encouragingly, the photo-cytotoxicity of **1a** is barely influenced, with IC_{50} of $2.93\ \mu\text{M}$ and $3.11\ \mu\text{M}$ in BSA-free and BSA-containing medium, respectively; that is, **1a** maintained 94 % of original cytotoxicity when facing a high blood concentration of BSA, which provides a strong indication of using the photo-activation strategy to control

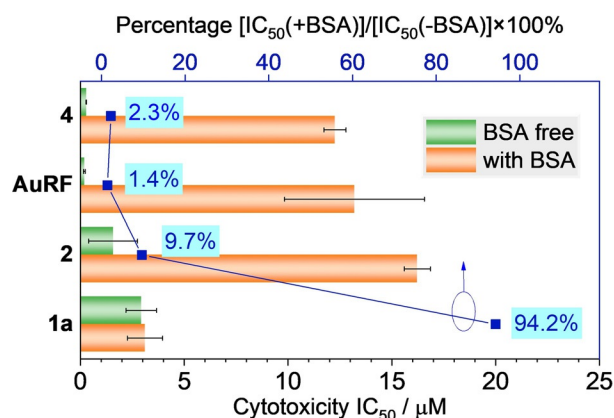


Figure 5. Cytotoxicity of gold complexes towards HepG2 cells in BSA-free and $40\ \text{mg mL}^{-1}$ BSA-containing minimal essential medium. AuRF = auranofin.

thiol-reactivity and to combat the drug deactivation issue caused by serum albumin. Interestingly, the cytotoxicity of **4** decreased heavily by BSA, possibly due to its characteristic non-covalent interactions.^[15b]

Inhibition of thiol-enzymes by gold complexes (e.g., gold(I)-alkyne, gold(I) phosphine) has been demonstrated to possibly induce anti-angiogenesis activity in vivo.^[3a,4g,26] We tested if the photo-activated gold(III)-hydride complex displays similar activity by using a transgenic GFP-Lc3 zebrafish model which shows green fluorescence in vasculature. The embryos were treated with **1a** for 1 h and then 420 nm light for 20 min. Four days later, impaired caudal artery (CA) and intersegmental vessels (IV) and absence of dorsal longitudinal anastomotic vessels (DLAV), particularly in the tail region, were found in the treatment group.

For comparison, the embryos treated with solvent control (Figure 6) or **1a** without light irradiation (Figure S19) did not show noticeable inhibition. In view that thiol-reactive gold(III) complexes, as compared to gold(I), have seldom been reported to display anti-angiogenesis activity in vivo, the activity of photo-activated **1a** implies reactive gold(III) species could act similarly to gold(I) for blood vessel inhibition in animal models.

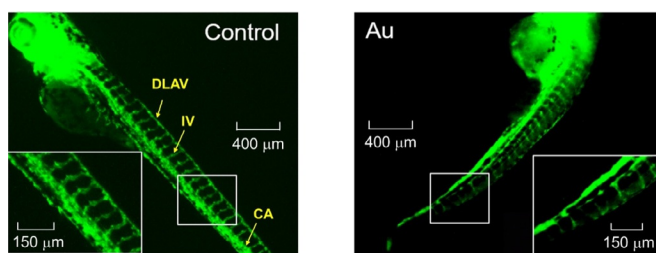


Figure 6. Formation of blood vessels during zebrafish embryo development. The transgenic embryos were treated with **1a** ($100 \mu\text{g L}^{-1}$) for 1 h followed by 420 nm light irradiation for 20 min. Blood vessels were monitored 4 days after fertilization. Left: solvent control; right: **1a**-treated.

Since the gold(III)-hydride complexes consist with cyclometalated donor-acceptor ligands and show strong charge transfer characters at the excited state (Figure 2), we estimate that these complexes could be activated by two-photon irradiation with long wavelength at the phototherapeutic window (650–1350 nm).^[27] Two-photon fluorescence microscopy analysis showed that the cytoplasmic fluorescence of **1b** in cancer cells can be efficiently excited with 690–700 nm laser light (Figure S20), the image of which is the same as the case by 405 nm excitation. By using a calcein AM/EthD-1 co-staining assay (Figure S21a), irradiation with 690–700 nm laser light for 5 min efficiently induced cell death, with phenomenon and activity similar to 405 nm irradiation. In the control group with laser irradiation only, no cell death was found (Figure S21b). These results indicate the gold(III)-hydride complexes are two-photon activatable, rendering the possibility to reach deep tumor tissues.

Conclusion

In summary, a series of cyclometalated gold(III)-hydride complexes has been identified to display photo-induced reactivity towards thiols, leading to potent inhibition of thioredoxin reductase with an up to >400-fold increase of cytotoxicity (vs. dark) and strong inhibition of angiogenesis on zebrafish embryos after one- or two-photon light activation. Notably, the gold(III)-hydride complexes did not undergo reduction reactions, but instead formed photo-substituted adducts with thiols, which could be attributed to the high reactivity and photo-lability of monohydride ligands.^[16] In the literature, both gold(I) and gold(III) complexes are well-known thiol-enzyme (e.g., TrxR) inhibitors, but few displays controllable thiol-reactivity to inhibit enzyme targets highly specifically in cancer cells. The photo-activatable gold(III)-hydride complexes in this study offer a possibility to, on the one hand, overcome the longstanding drug deactivation issue caused by serum albumin, and on the other hand to achieve high tumor specificity via spatial and temporal control of light irradiation. This study, as we believe, will pave the way for the design of gold-based therapeutics with high anti-tumor activity and low side effects.

Experimental Section

Details for synthesis and characterization of the gold(III)-hydride complexes, DFT and TD-DFT calculations, TrxR inhibition assay, cytotoxicity MTT assay, one-/two-photon laser fluorescence microscopy analysis, anti-angiogenesis experiment and live/dead co-staining experiments can be found in Supporting Information.

Zebrafish model was used in our study. The experiment was performed under the guideline of the Institutional Animal Care and Use Committee of Sun Yat-sen University.

Acknowledgements

We would like to thank Prof. Chi-Ming Che (HKU) and Dr. Chun-Nam Lok (HKU) for helpful discussion. We are also thankful to Prof. Huaiyi Huang (SYSU) for help in two-photon imaging experiment and Prof. Chuanhao Li (SYSU) for assistance in GC analysis. T.Z acknowledges the support from Guangdong Science and Technology Department (No. 2019QN01C125). This work was financially supported by the start-up funding of Sun Yat-Sen University, Fundamental Research Funds for the Central Universities, Guangdong Key Lab of Chiral Molecule and Drug Discovery (2019B030301005), Shenzhen Fundamental Research Fund JCYJ20180508163206306, the open project from the State Key Laboratory of Coordination Chemistry in Nanjing University, Guangdong Province Zhu Jiang Talents Plan (2016ZT06C090) and Guangzhou City Talents Plan (CYLJTD-201609). The Warshel Institute for Computational Biology funding from Shenzhen City and Longgang District is also acknowledged.

Conflict of interest

The authors declare no conflict of interest.

Keywords: anti-cancer · gold medicine · photoactivatable prodrug · thiol reactivity · thioredoxin reductase

- [1] a) C. F. Shaw, *Chem. Rev.* **1999**, 99, 2589–2600; b) I. Ott, *Coord. Chem. Rev.* **2009**, 253, 1670–1681; c) A. Casini, L. Messori, *Curr. Top. Med. Chem.* **2011**, 11, 2647–2660; d) S. J. Berners-Price, A. Filipovska, *Metallomics* **2011**, 3, 863–873; e) M. A. Cinellu, I. Ott, A. Casini in *Bioorganometallic Chemistry*, (Eds.: G. Jaouen, M. Salmann), Wiley, Hoboken, **2015**, pp. 117–140; f) T. Zou, C. T. Lum, C.-N. Lok, J.-J. Zhang, C.-M. Che, *Chem. Soc. Rev.* **2015**, 44, 8786–8801; g) B. Bertrand, M. R. M. Williams, M. Bochmann, *Chem. Eur. J.* **2018**, 24, 11840–11851.
- [2] a) A. M. Pizarro, A. Habtemariam, P. J. Sadler, *Top. Organomet. Chem.* **2010**, 32, 21–56; b) S. Nobili, E. Mini, I. Landini, C. Gabbiani, A. Casini, L. Messori, *Med. Res. Rev.* **2010**, 30, 550–580; c) S. P. Mulcahy, E. Meggers, *Top. Organomet. Chem.* **2010**, 32, 141–153; d) S. D. Köster, H. Alborzinia, S. Can, I. Kitanovic, S. Wölfl, R. Rubbiani, I. Ott, P. Riesterer, A. Prokop, K. Merz, N. Metzler-Nolte, *Chem. Sci.* **2012**, 3, 2062–2072; e) L. Oehninger, R. Rubbiani, I. Ott, *Dalton Trans.* **2013**, 42, 3269–3284; f) S. J. Berners-Price, P. J. Barnard, in *Ligand Design in Medicinal Inorganic Chemistry*, Wiley, Hoboken, **2014**, pp. 227–256; g) B. Bertrand, A. Casini, *Dalton Trans.* **2014**, 43, 4209–4219; h) C. Nardon, G. Boscutti, D. Fregona, *Anticancer Res.* **2014**, 34, 487–492; i) M. Frik, J. Fernández-Gallardo, O. Gonzalo, V. Mangas-Sanjuan, M. González-Alvarez, A. Serrano del Valle, C. Hu, I. González-Alvarez, M. Bermejo, I. Marzo, M. Contel, *J. Med. Chem.* **2015**, 58, 5825–5841; j) J. Fernández-Gallardo, B. T. Elie, T. Sadhukha, S. Prabha, M. Sanaú, S. A. Rotenberg, J. W. Ramos, M. Contel, *Chem. Sci.* **2015**, 6, 5269–5283.
- [3] a) A. Meyer, C. P. Bagowski, M. Kokoschka, M. Stefanopoulou, H. Alborzinia, S. Can, D. H. Vlecken, W. S. Sheldrick, S. Wölfl, I. Ott, *Angew. Chem. Int. Ed.* **2012**, 51, 8895–8899; *Angew. Chem.* **2012**, 124, 9025–9030; b) T. Zou, C.-N. Lok, P.-K. Wan, Z.-F. Zhang, S.-K. Fung, C.-M. Che, *Curr. Opin. Chem. Biol.* **2018**, 43, 30–36.
- [4] a) P. J. Barnard, L. E. Wedlock, M. V. Baker, S. J. Berners-Price, D. A. Joyce, B. W. Skelton, J. H. Steer, *Angew. Chem. Int. Ed.* **2006**, 45, 5966–5970; *Angew. Chem.* **2006**, 118, 6112–6116; b) J. L. Hickey, R. A. Ruhayel, P. J. Barnard, M. V. Baker, S. J. Berners-Price, A. Filipovska, *J. Am. Chem. Soc.* **2008**, 130, 12570–12571; c) F. Cisnetti, A. Gautier, *Angew. Chem. Int. Ed.* **2013**, 52, 11976–11978; *Angew. Chem.* **2013**, 125, 12194–12196; d) W. Liu, R. Gust, *Chem. Soc. Rev.* **2013**, 42, 755–773; e) T. Zou, C. T. Lum, S. S.-Y. Chui, C.-M. Che, *Angew. Chem. Int. Ed.* **2013**, 52, 2930–2933; *Angew. Chem.* **2013**, 125, 3002–3005; f) R. Visbal, M. C. Gimeno, *Chem. Soc. Rev.* **2014**, 43, 3551–3574; g) T. Zou, C. T. Lum, C.-N. Lok, W.-P. To, K.-H. Low, C.-M. Che, *Angew. Chem. Int. Ed.* **2014**, 53, 5810–5814; *Angew. Chem.* **2014**, 126, 5920–5924; h) C. Bazzicalupi, M. Ferraroni, F. Papi, L. Massai, B. Bertrand, L. Messori, P. Gratteri, A. Casini, *Angew. Chem. Int. Ed.* **2016**, 55, 4256–4259; *Angew. Chem.* **2016**, 128, 4328–4331; i) W. Liu, R. Gust, *Coord. Chem. Rev.* **2016**, 329, 191–213; j) B. Bertrand, M. A. O’Connell, Z. A. E. Waller, M. Bochmann, *Chem. Eur. J.* **2018**, 24, 3613–3622; k) M. Mora, M. C. Gimeno, R. Visbal, *Chem. Soc. Rev.* **2019**, 48, 447–462; l) C. Schmidt, L. Albrecht, S. Balasubramanian, R. Misgeld, B. Karge, M. Brönstrup, A. Prokop, K. Baumann, S. Reichl, I. Ott, *Metallomics* **2019**, 11, 533–545.
- [5] a) S. J. Berners-Price, C. K. Mirabelli, R. K. Johnson, M. R. Mattern, F. L. McCabe, L. F. Faucette, C.-M. Sung, S.-M. Mong, P. J. Sadler, S. T. Crooke, *Cancer Res.* **1986**, 46, 5486–5493; b) N. Pillarsetty, K. K. Katti, T. J. Hoffman, W. A. Volkert, K. V. Katti, H. Kamei, T. Koide, *J. Med. Chem.* **2003**, 46, 1130–1132.
- [6] C. H. Chui, R. S.-M. Wong, R. Gambari, G. Y.-M. Cheng, M. C.-W. Yuen, K.-W. Chan, S.-W. Tong, F.-Y. Lau, P. B.-S. Lai, K.-H. Lam, C.-L. Ho, C.-W. Kan, K. S.-Y. Leung, W.-Y. Wong, *Bioorg. Med. Chem.* **2009**, 17, 7872–7877.
- [7] a) V. Milacic, D. Chen, L. Ronconi, K. R. Landis-Piowar, D. Fregona, Q. P. Dou, *Cancer Res.* **2006**, 66, 10478–10486; b) C. Marzano, L. Ronconi, F. Chiara, M. C. Giron, I. Faustinielli, P. Cristofori, A. Trevisan, D. Fregona, *Int. J. Cancer* **2011**, 129, 487–496; c) M. R. M. Williams, B. Bertrand, D. L. Hughes, Z. A. E. Waller, C. Schmidt, I. Ott, M. O’Connell, M. Searcey, M. Bochmann, *Metallomics* **2018**, 10, 1655–1666.
- [8] K. Yan, C.-N. Lok, K. Bierla, C.-M. Che, *Chem. Commun.* **2010**, 46, 7691–7693.
- [9] a) S. H. C. Askes, A. Bahreman, S. Bonnet, *Angew. Chem. Int. Ed.* **2014**, 53, 1029–1033; *Angew. Chem.* **2014**, 126, 1047–1051; b) A. E. Pierri, D. A. Muizzi, A. D. Ostrowski, P. C. Ford, *Struct. Bonding (Berlin)* **2015**, 165, 1–45; c) L. N. Lameijer, D. Ernst, S. L. Hopkins, M. S. Meijer, S. H. C. Askes, S. E. Le Dévédec, S. Bonnet, *Angew. Chem. Int. Ed.* **2017**, 56, 11549–11553; *Angew. Chem.* **2017**, 129, 11707–11711; d) A. Li, C. Turro, J. J. Kodanko, *Chem. Commun.* **2018**, 54, 1280–1290; e) P. C. Ford, *Coord. Chem. Rev.* **2018**, 376, 548–564; f) L. N. Lameijer, C. van de Griend, S. L. Hopkins, A.-G. Volbeda, S. H. C. Askes, M. A. Siegler, S. Bonnet, *J. Am. Chem. Soc.* **2019**, 141, 352–362; g) H. Huang, S. Banerjee, K. Qiu, P. Zhang, O. Blacque, T. Malcomson, M. J. Paterson, G. J. Clarkson, M. Staniforth, V. G. Stavros, G. Gasser, H. Chao, P. J. Sadler, *Nat. Chem.* **2019**, 11, 1041–1048; h) V. H. S. van Rixel, V. Ramu, A. B. Auyeung, N. Beztsinna, D. Y. Leger, L. N. Lameijer, S. T. Hilt, S. E. Le Dévédec, T. Yildiz, T. Betancourt, M. B. Gildner, T. W. Hudnall, V. Sol, B. Liagre, A. Kornienko, S. Bonnet, *J. Am. Chem. Soc.* **2019**, 141, 18444–18454; i) C. Imberti, P. Zhang, H. Huang, P. J. Sadler, *Angew. Chem. Int. Ed.* **2020**, 59, 61–73; *Angew. Chem.* **2020**, 132, 61–73.
- [10] a) Y. Zhao, G. M. Roberts, S. E. Greenough, N. J. Farrer, M. J. Paterson, W. H. Powell, V. G. Stavros, P. J. Sadler, *Angew. Chem. Int. Ed.* **2012**, 51, 11263–11266; *Angew. Chem.* **2012**, 124, 11425–11428; b) S. Bonnet, *Dalton Trans.* **2018**, 47, 10330–10343; c) X. Xue, C. Qian, H. Fang, H.-K. Liu, H. Yuan, Z. Guo, Y. Bai, W. He, *Angew. Chem. Int. Ed.* **2019**, 58, 12661–12666; *Angew. Chem.* **2019**, 131, 12791–12796; d) X. Wang, X. Wang, S. Jin, N. Muhammad, Z. Guo, *Chem. Rev.* **2019**, 119, 1138–1192.
- [11] a) S. Betanzos-Lara, L. Salassa, A. Habtemariam, P. J. Sadler, *Chem. Commun.* **2009**, 6622–6624; b) F. Barragán, P. López-Senín, L. Salassa, S. Betanzos-Lara, A. Habtemariam, V. Moreno, P. J. Sadler, V. Marchán, *J. Am. Chem. Soc.* **2011**, 133, 14098–14108.
- [12] a) P. Müller, B. Schroder, J. A. Parkinson, N. A. Kratochwil, R. A. Coxall, A. Parkin, S. Parsons, P. J. Sadler, *Angew. Chem. Int. Ed.* **2003**, 42, 335–339; *Angew. Chem.* **2003**, 115, 349–353; b) N. J. Farrer, J. A. Woods, L. Salassa, Y. Zhao, K. S. Robinson, G. Clarkson, F. S. Mackay, P. J. Sadler, *Angew. Chem. Int. Ed.* **2010**, 49, 8905–8908; *Angew. Chem.* **2010**, 122, 9089–9092; c) Z. Wang, N. Wang, S.-C. Cheng, K. Xu, Z. Deng, S. Chen, Z. Xu, K. Xie, M.-K. Tse, P. Shi, H. Hirao, C.-C. Ko, G. Zhu, *Chem* **2019**, 5, 3151–3165; d) V. E. Y. Lee, C. F. Chin, W. H. Ang, *Dalton Trans.* **2019**, 48, 7388–7393.
- [13] a) S. Alonso-de Castro, E. Ruggiero, A. Ruiz-de-Angulo, E. Rezabal, J. C. Mareque-Rivas, X. Lopez, F. López-Gallego, L. Salassa, *Chem. Sci.* **2017**, 8, 4619–4625; b) S. Alonso-de Castro, A. L. Cortajarena, F. López-Gallego, L. Salassa, *Angew. Chem.*

- Int. Ed.* **2018**, *57*, 3143–3147; *Angew. Chem.* **2018**, *130*, 3197–3201.
- [14] a) R. W.-Y. Sun, C.-N. Lok, T. T.-H. Fong, C. K.-L. Li, Z. F. Yang, T. Zou, A. F.-M. Siu, C.-M. Che, *Chem. Sci.* **2013**, *4*, 1979–1988; b) T.-H. Fong, PhD thesis, The University of Hong Kong (Hong Kong), **2015**; c) S. Jürgens, V. Scalcon, N. Estrada-Ortiz, A. Folda, F. Tonolo, C. Jandl, D. L. Browne, M. P. Rigobello, F. E. Kühn, A. Casini, *Bioorg. Med. Chem.* **2017**, *25*, 5452–5460.
- [15] a) J. J. Yan, A. L.-F. Chow, C.-H. Leung, R. W.-Y. Sun, D.-L. Ma, C.-M. Che, *Chem. Commun.* **2010**, *46*, 3893–3895; b) S. K. Fung, T. Zou, B. Cao, P. Y. Lee, Y. M. E. Fung, D. Hu, C. N. Lok, C. M. Che, *Angew. Chem. Int. Ed.* **2017**, *56*, 3892–3896; *Angew. Chem.* **2017**, *129*, 3950–3954.
- [16] a) R. N. Perutz, B. Procacci, *Chem. Rev.* **2016**, *116*, 8506–8544; b) A. J. Jordan, G. Lalic, J. P. Sadighi, *Chem. Rev.* **2016**, *116*, 8318–8372; c) E. S. Wiedner, M. B. Chambers, C. L. Pitman, R. M. Bullock, A. J. M. Miller, A. M. Appel, *Chem. Rev.* **2016**, *116*, 8655–8692.
- [17] A. Pintus, L. Rocchigiani, J. Fernandez-Cestau, P. H. M. Budzelaar, M. Bochmann, *Angew. Chem. Int. Ed.* **2016**, *55*, 12321–12324; *Angew. Chem.* **2016**, *128*, 12509–12512.
- [18] Bochmann and co-workers have reported that the gold(III)-hydride analogue is stable towards HOAc in the dark. See: D.-A. Roşca, D. A. Smith, D. L. Hughes, M. Bochmann, *Angew. Chem. Int. Ed.* **2012**, *51*, 10643–10646; *Angew. Chem.* **2012**, *124*, 10795–10798.
- [19] In this work, the light intensities for each wavelength are fixed: $\lambda = 365$ nm, 6.87 mW cm^{-2} ; $\lambda = 420$ nm, 11.10 mW cm^{-2} ; $\lambda = 460$ nm, 23.88 mW cm^{-2} .
- [20] G. R. Fulmer, A. J. M. Miller, N. H. Sherden, H. E. Gottlieb, A. Nudelman, B. M. Stoltz, J. E. Bercaw, K. I. Goldberg, *Organometallics* **2010**, *29*, 2176–2179.
- [21] S. M. Barrett, C. L. Pitman, A. G. Walden, A. J. M. Miller, *J. Am. Chem. Soc.* **2014**, *136*, 14718–14721.
- [22] a) W.-P. To, G. S.-M. Tong, W. Lu, C. Ma, J. Liu, A. L.-F. Chow, C.-M. Che, *Angew. Chem. Int. Ed.* **2012**, *51*, 2654–2657; *Angew. Chem.* **2012**, *124*, 2708–2711; b) M.-C. Tang, A. K.-W. Chan, M.-Y. Chan, V. W.-W. Yam, *Top. Curr. Chem.* **2016**, *374*, 46; c) W.-P. To, G. S. M. Tong, C.-W. Cheung, C. Yang, D. Zhou, C.-M. Che, *Inorg. Chem.* **2017**, *56*, 5046–5059.
- [23] A. Bindoli, M. P. Rigobello, G. Scutari, C. Gabbiani, A. Casini, L. Messori, *Coord. Chem. Rev.* **2009**, *253*, 1692–1707.
- [24] J. F. R. Kerr, A. H. Wyllie, A. R. Currie, *Br. J. Cancer* **1972**, *26*, 239–257.
- [25] T. Mosmann, *J. Immunol. Methods* **1983**, *65*, 55–63.
- [26] I. Ott, X. Qian, Y. Xu, D. H. W. Vlecken, I. J. Marques, D. Kubutat, J. Will, W. S. Sheldrick, P. Jesse, A. Prokop, C. P. Bagowski, *J. Med. Chem.* **2009**, *52*, 763–770.
- [27] a) A. M. Smith, M. C. Mancini, S. Nie, *Nat. Nanotechnol.* **2009**, *4*, 710–711; b) M. C.-L. Yeung, V. W.-W. Yam in *Luminescent and Photoactive Transition Metal Complexes as Biomolecular Probes and Cellular Reagents* (Ed.: K. K.-W. Lo), Springer Berlin Heidelberg, Berlin, **2015**, pp. 109–129; c) Y. Chen, R. Guan, C. Zhang, J. Huang, L. Ji, H. Chao, *Coord. Chem. Rev.* **2016**, *310*, 16–40; d) F. Heinemann, J. Karges, G. Gasser, *Acc. Chem. Res.* **2017**, *50*, 2727–2736.

Manuscript received: January 11, 2020

Revised manuscript received: February 14, 2020

Accepted manuscript online: March 24, 2020

Version of record online: April 24, 2020